

**PREPARATION, CHARACTERIZATION AND PERFORMANCE OF  
POLYANILINE-TITANIUM OXIDE COMPOSITE PELLET FOR  
DETECTION OF ACETONE VAPOR**

**RAIHANA BINTI BAHRU**

**UNIVERSITI SAINS MALAYSIA**

**2013**

**PREPARATION, CHARACTERIZATION AND PERFORMANCE OF  
POLYANILINE-TITANIUM OXIDE COMPOSITE PELLET FOR  
DETECTION OF ACETONE VAPOR**

**by**

**RAIHANA BINTI BAHRU**

**Thesis submitted in fulfillment of the requirements for the degree  
of Master of Science**

**JULY 2013**

## ACKNOWLEDGEMENTS

In the name of Allah, the Most Gracious and the Most Merciful.

Alhamdulillah, all praises to Allah for His blessing and willness in completing this thesis. I would like to send my warmest appreciations to my supervisor, Associate Professor Dr. Mohamad Zailani Abu Bakar, for his continuous support and guidance of knowledge. There are numbered contributions of his constructive comments and unlimited suggestions throughout the experimental works and thesis which are helpful and inspired.

I would like to extend my appreciations to the Dean School of Chemical Engineering, Professor Azlina binti Harun @ Kamaruddin and also the Deputy Dean of School of Chemical Engineering, Associate Professor Dr. Ahmad Zuhairi Abdullah, for their support and management towards my postgraduate affairs. The list of my acknowledgements goes to all the lecturers and staffs of School of Chemical Engineering, USM for their co-operations and continuity support. Not forgotten to the laboratory technicians especially Mr. Shamsul Hidayat Shaharan and Mr. Arif for their technical assistance during laboratory work.

I would like to thank the Universiti Sains Malaysia, USM for providing me the USM Fellowship Scheme during my studies for financial support as well as the allocation for funding this research through SCIENCEFUND grant. Sincere appreciations to all my beloved friends especially Kak jusliha, Syazwina, Ashikin, Khadijah, Kak Min, Kak Syria, Guat Wei, Ummi Haiza for their kindness and moral support during my study.

Last but not least, I dedicate my heartiest gratitude to my adored parents, Mr. Bahru bin Abu Bakar and Mrs. Sarimah binti Haron and also to my siblings for their endless love, prayers and encouragement. Also to my beloved husband, Mohd Faiz Muaz bin Ahmad Zamri for his encouragement, endless love, prayers and support for my study. Finally, thanks to those who have indirectly contributed to this research. Thank you very much.

*-Raihana Bahru, July 2013-*

## TABLE OF CONTENTS

	Page
<b>ACKNOWLEDGEMENTS</b>	ii
<b>TABLE OF CONTENTS</b>	iv
<b>LIST OF TABLES</b>	viii
<b>LIST OF FIGURES</b>	ix
<b>LIST OF PLATES</b>	xii
<b>LIST OF ABBREVIATIONS</b>	xiii
<b>LIST OF SYMBOLS</b>	xv
<b>ABSTRAK</b>	xvi
<b>ABSTRACT</b>	xviii
<b>CHAPTER 1- INTRODUCTION</b>	
1.1 Acetone	1
1.1.1 Definition	1
1.1.2 Sources of Acetone Emission	2
1.1.3 Level of Risk and Environmental Impact	4
1.2 Type of Gas Sensor	4
1.2.1 Semiconductor Gas Sensor	5
1.2.2 Conducting Polymer Gas Sensor	5
1.3 Problem Statement	6
1.4 Objectives	7
1.5 Scope of Study	8
1.6 Organization of The Thesis	9
<b>CHAPTER 2- LITERATURE REVIEW</b>	
2.1 Introduction	11
2.2 Semiconductor Metal Oxide Gas Sensor	11
2.3 Gas Sensing Mechanism	14
2.4 Composite Semiconductor Gas Sensor	17
2.4.1 Metal-Metal Oxide Gas Sensor	17

2.4.2	Mixed Metal Oxide	18
2.4.3	Polymer-Metal or Metal Oxide	19
2.5	Conducting Polymer Loadings on Metal Oxide	20
2.5.1	Polyaniline	20
2.5.2	Polypyrrole	21
2.6	Structure and Properties of PANI-TiO <sub>2</sub> Composite Gas Sensor	22
2.6.1	Surface Morphology and Chemical Bonding	22
2.6.2	Resistance Temperature Characteristics	25
2.7	Method for Preparation of Pellet Gas Sensor	26
2.7.1	In-situ Chemical Polymerization	26
2.7.2	Electrochemical Deposition	27
2.8	Concluding Remarks	28

### **CHAPTER 3- MATERIALS AND METHODS**

3.1	Introduction	30
3.2	Materials and Chemical Reagents	32
3.3	Equipment	33
3.4	PANI-TiO <sub>2</sub> Composite Pellet Preparation	34
3.5	PANI-TiO <sub>2</sub> Composite Pellet Characterization	37
3.5.1	X-ray Diffraction (XRD)	37
3.5.2	Scanning Electron Microscopy (SEM)	38
3.5.3	Energy Dispersive X-ray (EDX) Spectroscopy	38
3.5.4	Transmission Electron Microscopy (TEM)	38
3.5.5	Fourier Transformation Infrared Spectroscopy (FTIR)	39
3.5.6	Surface Analysis (N <sub>2</sub> Adsorption-desorption)	39
3.6	PANI-TiO <sub>2</sub> Composite Pellet Sensing Performance Testing	40
3.6.1	Experimental Rig Set-up	40
3.6.2	Calibration of Gas Concentration	41
3.6.3	Experimental Procedures	42
3.6.4	Sensor Activity Measurement	43
3.7	Parameter Studies	45
3.7.1	Parameter Studies in Preparation of Sensing Material	45

3.7.2	Parameter Studies in Acetone Sensing Activity	45
3.7.2	(a) Effect of Operating Temperature	45
3.7.2	(b) Effect of Acetone Vapor Concentration	46
3.8	Optimization Studies	46

## **CHAPTER 4- RESULTS AND DISCUSSION**

4.1	Introduction	49
4.2	Characterization	50
4.2.1	X-ray Diffraction (XRD)	50
4.2.2	Scanning Electron Microscopy (SEM)	55
4.2.3	Energy Dispersive X-ray (EDX)	57
4.2.4	Transmission Electron Microscopy (TEM)	59
4.2.5	Fourier Transformation Infrared Spectroscopy (FTIR)	61
4.2.6	Surface Analysis (N <sub>2</sub> adsorption-desorption)	64
4.3	Gas Sensitivity Performance	68
4.3.1	Resistance-temperature Characteristic	68
4.4	Performance of Pellet Gas Sensor Under Various Operating Conditions	74
4.4.1	Effect of operating temperature	74
4.4.2	Effect of Different Concentration of Acetone Vapor	78
4.5	Optimum Condition using Design of Experiment (DOE)	81
4.5.1	Response Surface Methodology (RSM)	81
4.5.2	Analysis of Variance (ANOVA)	83
4.5.3	Model Analysis	85
4.6	Performance of selected pellet gas sensor under optimum operating conditions	88
4.6.1	Effect of Operating Temperature	89
4.6.2	Effect of Different Concentration of Acetone Vapor	89

## **CHAPTER 5- CONCLUSION AND RECOMMENDATIONS**

5.1	Conclusion	92
-----	------------	----

5.2 Recommendations for Future Work	94
<b>REFERENCES</b>	95
<b>APPENDICES</b>	
Appendix A: Gas chromatogram (GC) for acetone vapor.	106
Appendix B: Example of calculation for the preparation of acetone standards and sample in GC.	107
<b>LIST OF PUBLICATIONS</b>	109

## LIST OF TABLES

		Page
Table 2.1	Sign of resistance change (increase or decrease) to change in gas atmosphere (William, 1999).	12
Table 2.2	Summary of conducting polymer – metal oxides used in gas sensing applications.	29
Table 3.1	List of materials and chemicals used.	32
Table 3.2	List of equipment used.	33
Table 3.3	Experimental matrix for central composite design (CCD) for the optimization of composite sensor pellet detection.	47
Table 3.4	Independent variables: coded and actual values of variables of the design of experiments for the optimization of composite sensor pellet detection.	48
Table 4.1	Crystallite size of the pure TiO <sub>2</sub> , pure PANI and 20wt.% PANI-TiO <sub>2</sub> composite pellet.	55
Table 4.2	Elemental composition of pure TiO <sub>2</sub> and PANI-TiO <sub>2</sub> composite pellet.	58
Table 4.3	Textural properties of pure TiO <sub>2</sub> and loadings-modified TiO <sub>2</sub> powders with different loadings.	68
Table 4.4	Sensitivity performance for different loadings of PANI-TiO <sub>2</sub> composite at 27°C of operating temperature and 100 ppm acetone vapor concentration.	76
Table 4.5	Experimental design results for performance of PANI-TiO <sub>2</sub> composite pellet.	82
Table 4.6	ANOVA for the regression model and the respective model terms for performance of PANI-TiO <sub>2</sub> composite pellet.	84
Table 4.7	Error of sensitivity performance of PANI-TiO <sub>2</sub> composite pellet gas sensor for detection at 45°C and 300 ppm concentration of acetone vapor.	90
Table B1	Calculation of acetone vapour.	107

## LIST OF FIGURES

		Page
Figure 1.1	Global acetone emission in 1994, Singh <i>et al</i> , 1994.	3
Figure 2.1	Schematic band diagrams of an insulator, semi-conductor and conductor. Note the small gap in the semiconductor, where electrons with sufficient energy can cross and the overlapping of the bands in the conductor (Shriver, 2006).	13
Figure 2.2	Surface conductance effect (Spetz, 2006).	15
Figure 2.3	Bulk conductance effect (Spetz, 2006).	15
Figure 2.4	Schematic diagram of the sensing mechanism of the metal oxide semiconductor gas sensor (Spetz, 2006).	16
Figure 2.5	Protonated emeraldine obtained after the polymerization of aniline can be oxidized to pernigraniline or reduced to leucoemeraldine. Emeraldine and pernigraniline may be deprotonated to the corresponding bases. Adapted from (Stejskal <i>et al</i> , 1996).	21
Figure 2.6	SEM image for (a) Pure PANi and (b) PANi:TiO <sub>2</sub> particles. (Tai <i>et al.</i> , 2008).	23
Figure 2.7	TEM images for (a) pure TiO <sub>2</sub> , (b) pure PANI, (c) PANI/TiO <sub>2</sub> composite (Srivasta <i>et al</i> , 2011).	24
Figure 2.8	FTIR spectra of PANI/TiO <sub>2</sub> composites with different contents of (a) 0, (b) 5, (c) 25, (d) 50, and (e) 80 wt.% (Xu <i>et al</i> , 2005).	25
Figure 3.1	Flowchart diagram of overall process study.	32
Figure 3.2	Flow chart of experimental procedure for synthesis of the PANI-TiO <sub>2</sub> composite pellet.	35
Figure 3.3	Mould geometry dimension.	36
Figure 3.4	Diagram of sensing measurement unit.	41
Figure 3.5	Schematic series circuit for R-V electronic circuit.	44
Figure 4.1	XRD patterns of pure TiO <sub>2</sub> , pure PANI and 20wt.% PANI-TiO <sub>2</sub> composite powder. A = anatase      R = rutile	52
Figure 4.2	XRD patterns of 20, 25, 30, 35 and 40wt.% PANI-TiO <sub>2</sub> composite powder. A = anatase      R = rutile	53

Figure 4.3	SEM images of (a) pure TiO <sub>2</sub> , (b) pure PANI, (c) 20wt.% PANI-TiO <sub>2</sub> , (d) 30wt.% PANI-TiO <sub>2</sub> , (e) 40wt.% PANI-TiO <sub>2</sub> .	56
Figure 4.4	EDX spectrum of (a) pure TiO <sub>2</sub> , (b) pure PANI and (c) 20wt.% PANI-TiO <sub>2</sub> composite pellet.	58
Figure 4.5	TEM images (a) pure TiO <sub>2</sub> , (b) pure PANI, (c) 20wt.% PANI-TiO <sub>2</sub> , (d) 30wt.% PANI-TiO <sub>2</sub> , and (e) 40wt.% PANI-TiO <sub>2</sub> composite pellet.	60
Figure 4.6	FTIR spectra of (a) pure PANI and (b) 20wt.% PANI-TiO <sub>2</sub> composite pellet.	62
Figure 4.7	FTIR spectra of (a) 40wt.%, (b) 35wt.%, (c) 30wt.%, (d) 25wt.% and (e) 20wt.% PANI-TiO <sub>2</sub> composite pellet.	63
Figure 4.8	N <sub>2</sub> adsorption-desorption isotherms of pure TiO <sub>2</sub> and PANI-TiO <sub>2</sub> powders.	65
Figure 4.9	N <sub>2</sub> adsorption-desorption isotherms of PANI-TiO <sub>2</sub> powders with different PANI loadings.	66
Figure 4.10	Pore size distributions of 20wt.% PANI-TiO <sub>2</sub> composite.	67
Figure 4.11	Electrical resistance of 20wt.% PANI-TiO <sub>2</sub> composite pellet in purified air as compared with that of the pure TiO <sub>2</sub> pellet.	69
Figure 4.12	Electrical resistance of PANI-TiO <sub>2</sub> composite pellets in purified air at different PANI loadings.	70
Figure 4.13	Comparison of sensitivity performance between pure TiO <sub>2</sub> pellet and 20wt.% PANI-TiO <sub>2</sub> composite pellet at various operating temperature.	75
Figure 4.14	Comparison of sensitivity performance between different loading of PANI towards TiO <sub>2</sub> composite pellet at various operating temperature and 100ppm concentration of acetone vapor.	78
Figure 4.15	Sensing performance of pure TiO <sub>2</sub> and 20wt.% PANI-TiO <sub>2</sub> composite pellets in purified air for various concentration of acetone vapor, 27°C of operating temperature.	79
Figure 4.16	Sensing performance of PANI-TiO <sub>2</sub> composite pellets in purified air at different PANi addition for various concentration of acetone vapor, 27°C of operating temperature.	80

Figure 4.17	Parity plot for the experimental % sensitivity of PANI-TiO <sub>2</sub> composite pellet and the % sensitivity predicted value from equation 4.12.	85
Figure 4.18	Main effects plot of three significant factors for % Sensitivity of PANI-TiO <sub>2</sub> composite pellet. Conditions: Temperature: 27 - 65°C, gas (acetone) concentration: 100 – 300 ppm, % Composite: 20 – 40wt.%.	86
Figure 4.19	Interaction plot of temperature and gas concentration at 30wt.% PANI-TiO <sub>2</sub> composite pellet.	87
Figure 4.20	Three-dimension response surface contour plot indicating the effect of interaction between temperature and gas concentration for 30% PANI-TiO <sub>2</sub> composite.	88
Figure 4.21	Sensitivity of 30wt.% PANI-TiO <sub>2</sub> composite pellet at various operating temperature for 300 ppm acetone vapour concentration.	89
Figure 4.22	Sensitivity performance of 30wt.% PANI-TiO <sub>2</sub> composite pellet at various acetone vapor concentrations for operating temperature of 45°C.	90
Figure A1	Typical gas chromatogram fo sample of acetone vapor.	106
Figure B1	Calibration curve for acetone vapour.	108

## LIST OF PLATES

		Page
Plate 3.1	Stainless steel mould used for pellet preparation.	36
Plate 3.2	Manual hydraulic press.	37
Plate 3.3	Keithley's 5 1/2-digit model 6517A electrometer.	43

## LIST OF ABBREVIATIONS

Ag	Silver
ANI	Aniline
ANNOVA	Analysis of variance
APS	Ammonium persulfate
Au	Gold
BET	Brunauer – Emmett – Teller
BJH	Barret-Joyner-Halenda
C	Carbon
C4	Carbon 4
C6	Carbon 6
C <sub>6</sub> H <sub>5</sub> NH <sub>2</sub>	Aniline
CCD	Central composite design
CCFD	Central Composite Face-Centered Design
CH <sub>3</sub> COCH <sub>3</sub>	Acetone
CH <sub>3</sub> COOH	Acetic acid
CO	Carbon monoxide
CO <sub>2</sub>	Carbon dioxide
CO <sub>3</sub> O <sub>4</sub>	Cobalt (IV) oxide
Cr <sub>2</sub> O <sub>3</sub>	Chromium oxide
DOE	Design of experiment
EDX	Energy dispersion X-ray
Fe <sub>2</sub> O <sub>3</sub>	Ferric oxide / Iron oxide
FID	Flame ionisation detector
FTIR	Fourier Transformation Infrared
H <sub>2</sub>	Hydrogen
H <sub>2</sub> O	Water
HCl	Hydrochloric acid
JCPDS	Joint Committee on Powder Diffraction Standard
ICCD	International Centre for Diffraction Data
In <sub>2</sub> O <sub>3</sub>	Indium oxide
KBr	Kalium bromate
MoO <sub>3</sub>	Molibdenum oxide

MOS	Metal oxide gas sensor
N <sub>2</sub>	Nitrogen
NDIR	Non-dispersive infrared sensor
NH <sub>3</sub>	Ammonia
NiCr	Nickel chromium
NiO	Nickel oxide
O <sub>2</sub>	Oxygen
OH	Hydroxide
PANI	Polyaniline
Pd	Palladium
PID	Photo ionisation detector
PM-10	Particulate matter 10 ppm
PM-2.5	Particulate matter 2.5 ppm
PPy	Polypyrrole
Pt	Platinum
PTh	Polythiophene
RSM	Response Surface Methodology
R-V	Resistance-voltage
SEM	Scanning electron microscopy
SGS	Semiconductor gas sensor
SiO <sub>2</sub>	Silicon dioxide
SnO <sub>2</sub>	Tin oxide
TEM	Transmission electron microscopy
TiO <sub>2</sub>	Titanium oxide
VOCs	Volatile organic compounds
WO <sub>3</sub>	Tungsten
XRD	X-ray diffraction
ZnO	Zinc oxide

## LIST OF SYMBOLS

Symbols	Description	Unit
°C	Degree celcius	Dimensionless
A, B or C	Coded factors	Dimensionless
cp	Centipoise	mPa.s
eV	Energy barrier	kJ/mol
M	Concentration	Molar
R, R <sub>air</sub> , R <sub>acetone</sub>	Electrical resistance	Ohm ( $\Omega$ )
R <sup>2</sup>	Coefficient of determination	Dimensionless
S	Sensitivity	Dimensionless
Symbols	Description	Unit
T	Temperature	K
V	Voltage	Volt
v/v	Volume ratio	Dimensionless
wt. %	Weight percentage	Dimensionless
$\beta$	Full width at half maximum (FWHM)	Dimensionless
$\theta$	Bragg angle	Dimensionless
$\lambda$	Wavelength of Cu-K $\alpha$	Dimensionless

# **PENYEDIAAN, PENCIRIAN DAN PRESTASI PELET KOMPOSIT POLIANILIN-TITANIUM OKSIDA BAGI PENGESANAN WAP ASETON**

## **ABSTRAK**

Kajian ini memfokuskan ke atas pengesanan sebatian organik meruap dengan tumpuan khas ke atas aseton yang berbahaya kepada persekitaran dan kesihatan manusia. Pengesan asas semikonduktor adalah salah satu pengesan sebatian organik meruap yang terbaik yang sedia ada. Walaubagaimanapun, kekurangan utama pengesan jenis ini adalah penggunaan suhu operasi optima yang tinggi (lebih besar daripada 200°C). Pendekatan yang menarik untuk menurunkan suhu operasi adalah dengan menambahkan bahan organik sebagai bahan pengesan tambahan. Suatu polimer berkonduktor yang dikenali sebagai polianilin (PANI) telah ditambah kepada titanium oksida (TiO<sub>2</sub>) dengan menggunakan kaedah in-situ pempolimeran kimia untuk membentuk pelet komposit PANI-TiO<sub>2</sub> bagi pengesanan wap aseton. Pengesan komposit tersebut telah dicirikan menggunakan belauan sinar-X (XRD), mikroskop elektron imbasan (SEM) dan spektroskop penyebaran tenaga sinar-X (EDX), mikroskop elektron imbasan (TEM), spektroskop infra merah pemindahan forier (FTIR) dan analisis permukaan (penyerapan-penyahserapan N<sub>2</sub>). Prestasi komposit pengesan telah diuji menggunakan unit pengukuran pengesan pada suhu 27°C - 65°C dengan melepaskan wap aseton pada pelbagai kepekatan dalam julat 100 – 500 ppm. Kaedah permukaan tindakbalas (RSM) telah digunakan untuk mengoptimumkan data eksperimen. Hubungkait antara 3 pembolehubah iaitu bahan tambah, suhu operasi dan kepekatan wap aseton telah dipertimbangkan. Didapati bahawa komposit terbaik yang memberikan pengesanan maksima adalah 30wt.% PANI-TiO<sub>2</sub>. Pengesanan optima adalah pada suhu operasi 45°C dengan anggaran pengesanan ~16.19% terhadap 300 ppm kepekatan wap aseton. Keputusan ujikaji telah membuktikan

bahawa kombinasi antara PANI dan  $\text{TiO}_2$  boleh menurunkan suhu operasi secara mendadak menghampiri suhu bilik.

# **PREPARATION, CHARACTERIZATION AND PERFORMANCE OF POLYANILINE-TITANIUM OXIDE COMPOSITE PELLET FOR DETECTION OF ACETONE VAPOR**

## **ABSTRACT**

The present work focuses on the detection of the VOCs with particular emphasis on acetone which is harmful to the environment and human health. The semiconductor based sensor is one of the best VOC sensors which currently available. However, the main drawback of this type of gas sensor is the utilization of high optimum operating temperature (greater than 200°C). An interesting approach for lowering the operating temperature is by incorporating an organic material as the additional sensing material. A conducting polymer known as polyaniline (PANI) was added to titanium oxide (TiO<sub>2</sub>) by in-situ chemical polymerization method to form PANI-TiO<sub>2</sub> composite pellet to be used for detection of acetone vapor. The composite sensor was characterized using X-ray Diffraction (XRD), Scanning Electron Microscopy (SEM) and Energy Dispersive X-ray (EDX) Spectroscopy, Transmission Electron Microscopy (TEM), Fourier Transformation Infrared Spectroscopy (FTIR), and Surface Analysis (N<sub>2</sub> adsorption-desorption). The performances of composite pellets were tested using sensing measurement unit at temperature 27°C - 65°C by releasing the acetone vapor at various concentrations in the range of 100 – 500 ppm. Response Surface Methodology (RSM) was used to optimize the experimental data. A correlation of 3 parameters which are additive loadings, operating temperature and acetone vapor concentration has been considered. It was found that 30wt.% PANI-TiO<sub>2</sub> was the best composite pellet which gave the maximum sensitivity. The optimum performance was at 45°C with sensitivity approximately at ~16.19% towards 300 ppm acetone vapor concentration.

The experimental results proved that the combination between PANI and TiO<sub>2</sub> could significantly reduce the operating temperature as low as the room temperature.

# CHAPTER 1

## INTRODUCTION

The overloading of air pollution issues is increasing throughout the year among the developed countries. The major sources of air pollution come from motor vehicles, power plants and industrial facilities, agricultural operations, mining and open burning. The most common and damaging pollutants from these sources include sulfur dioxide, suspended particulate matter (PM-10 and PM-2.5), nitrogen dioxide, ground-level ozone, carbon monoxide and volatile organic compounds (VOCs).

The present study concentrates on the detection of the VOCs with particular emphasis on acetone which is harmful to the environment and affects human health. Matters related to acetone are briefly discussed in the following sections, followed by the brief detection methodology and finally lead to the problem statement and the objectives of the present study.

### 1.1 Acetone

#### 1.1.1 Definition

Acetone with a chemical formula of  $\text{CH}_3\text{COCH}_3$  has a relative molecular mass of 58.08 g/mole and is classified as ketone which is one of the types of organic solvent. It is a clear, colorless liquid with a sweet smell and distinctive taste, which easily evaporates at ambient temperatures. Although acetone is an excellent solvent, it is extremely flammable (flash point  $-17^\circ\text{C}$  closed cup;  $-9^\circ\text{C}$  open cup; flammability limits in air at  $25^\circ\text{C} = 2.15\text{-}13\% \text{ v/v}$ ). The low viscosity (0.303 cp at  $25^\circ\text{C}$ ), high

evaporation rate (vapour pressure 181.72 mmHg at 20°C), and miscibility of acetone make it a useful solvent. In fact, it is miscible with water and other organic solvents (Minnesota department health: Indoor Air Unit, Minnesota Department of Health Fact Sheet, 2010).

Acetone is mainly used in processes as both solvent and intermediate in chemical production. Those processes which involve acetone either as a product or by-product have contributed to the high impact of reaction with air and consequently leading to air pollution. Therefore, proper management and authorization on the emission of acetone are highly necessary and should be carried out in accordance to the standard regulation issued by the health association.

### **1.1.2 Sources of Acetone Emission**

According to Singh *et al.* (1994), the global emissions of acetone are estimated at 40 to 60 Tg ( $10^{12}$  g) per year. Of this amount, the secondary formation of acetone is estimated to contribute approximately 50% of these emissions. Biomass burning, direct biogenic emissions and primary anthropogenic emissions contribute to 26%, 21% and 3% of global acetone emissions, respectively (Singh *et al.*, 1994).

Acetone is emitted mostly in gaseous form instead of liquid. The emission of acetone vapor is much more difficult to handle compared to liquid acetone where the acetone is rapidly converted into vapor phase at atmospheric condition. Atmospheric emissions occur from consumer products including nail, polish removers, particle board, carpet backing, some paint removers, and liquid/paste waxes or polishes. It is also found in detergents/cleansers, adhesives, and automobile carburetor and choke cleaners.

Acetone is also produced in the atmosphere by photooxidation of compounds such as propane, propylene oxide, epichlorohydrin, mycene, and other C4 to C6 alkenes (Janson and de Serves, 2001). A report from Singh *et al.* (1994) found acetone in a range of approximately  $\sim 0.9\text{-}5.2 \mu\text{g}/\text{m}^3$  (approx. 0.4-2.3 ppb), with a mean of  $3.1 \mu\text{g}/\text{m}^3$  (1.14 ppb), in the troposphere. Figure 1.1 shows the greatest source of acetone is the oxidation of precursor hydrocarbons (51%); other sources are biomass burning (26%), biogenic emissions (21%) and an anthropogenic emission (approx. 2%). Atmospheric removal is mainly by photolysis (64%), followed by reaction with  $\text{OH}^*$  radicals (24%) and deposition (12%).

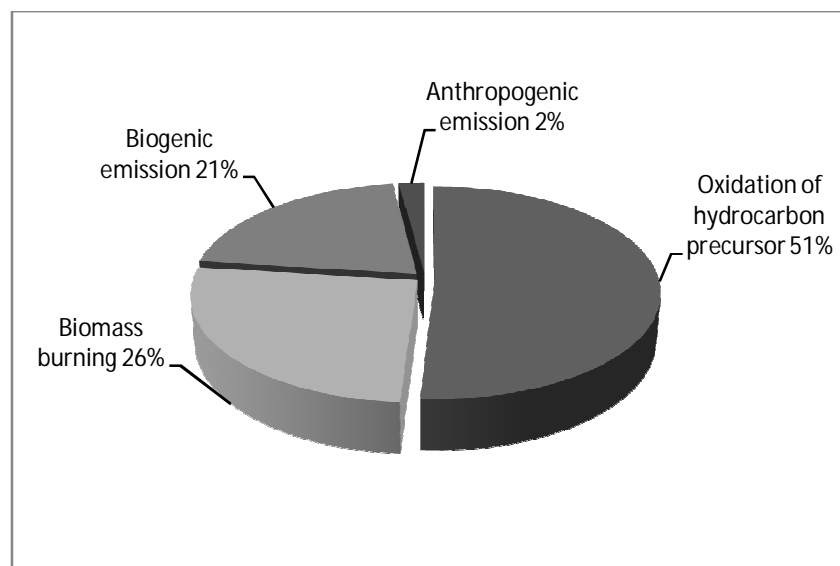


Figure 1.1: Global acetone emission in 1994 (Source: Singh *et al.*, 1994)

Other natural sources of acetone air emissions include vegetation (mainly evergreens), volcanic eruptions, forest fires, and oceans. In addition, the anthropogenic emission sources of acetone include chemical and manufacturing industries, vehicle exhaust, biomass and plastic burning, pulping, refuse combustion, tobacco smoke, petroleum production and landfills.

### **1.1.3 Level of Risk and Environmental Impact**

Acetone is typically a non-acutely toxic, however it has compound that can affect long-term health which is commonly found in volatile contaminant. Exposure to 250 ppm for 4 hours has caused mild effects on the performance in some behavioral tests such as auditory tone discrimination and a mood test. As the concentration approaches 1000 ppm, noticeable irritation has occurred and some people have reported encountering headaches, light-headedness and tiredness. Inhalation of concentrations higher than 2000 ppm can cause dizziness, a feeling of intoxication, drowsiness, nausea and vomiting.

Unconsciousness may also result if the exposure is extremely higher (greater than 10000 ppm). Intolerable nose and throat irritation would also occur at these levels of concentrations. Even, higher concentrations can cause collapse, coma and death. Due to its health effects in nature, it is crucial that acetone concentration should be properly monitored by using suitable gas sensors (Material Safety Data Sheet of Acetone, Sunoco, Inc. (R&M); Environmental Health Criteria 207, 1998).

## **1.2 Type of Gas Sensor**

There are several well-established types of gas sensors for detection of VOCs in industries such as a flame ionization detector (FID), non-dispersive infrared sensor (NDIR), photo ionization detector (PID), infrared spectrophotometry, electrochemical sensor, catalytic sensor, metal oxide semiconductor, gold film (mercury), detector tubes and portable gas chromatography (OSHA, 2009).

Among the sensors metal oxide based semiconductor gas sensor is found to have good performance in detection of toxic pollutant and the dominance of industrial processes (Arshak and Gaiden, 2005). This is due to the good behavior of metal oxide semiconductor gas sensor towards sensing performance such as small grain size, low energy consumption and higher surface area to volume ratio (Carotta *et al.*, 1999; Zhao *et al.*, 2002; Yamazoe *et al.*, 2003; Arshad *et al.*, 2008).

### **1.2.1 Semiconductor Gas Sensor**

Semiconductor gas sensor (SGS) or also known as a chemoresistive gas sensor, basically is a response on the modification of electrical conductivity of the nanocomposite films ( $\text{TiO}_2$ ,  $\text{SnO}_2$ ,  $\text{WO}_3$ ,  $\text{ZnO}$  and  $\text{In}_2\text{O}_3$ ) due to the adsorbed gas species. Most of these devices give good performance at optimum conditions where the attributes of metal oxide gas sensor are well-established in fulfilling the requirement of gas sensor for industries (Tai *et al.*, 2010).

Semiconductor effect is perhaps the most attractive measurable responses since it gives very accurate readings. The fabrication of semiconductor gas sensor contributes the deposition of nanocomposite films onto a substrate provided with interdigital electrodes made from either Pt or Au. The resistance of the nanocomposite film is monitored when the film or pellet is exposed to different gases (Kickelbick, 2007).

### **1.2.2 Conducting Polymer Gas Sensor**

Conducting polymers, such as polypyrrole (PPy), polyaniline (PANI), polythiophene (PTh) and their derivatives have been used as the active layers of gas

sensors since early 1980s. The hybrid sensor with conducting polymer usually improves the behavior for most of the commercially available sensors which operate at high temperatures. Conducting polymer based gas sensors have high sensitivity and short response time particularly at lower operating temperatures. Besides, they are easy to be synthesized through chemical or electrochemical processes. The molecular chain structures can be modified conveniently by copolymerization or structural derivations provided they have good mechanical properties which allow a facile fabrication of sensors.

As a result, more and more attentions have been given to the sensors fabricated from conducting polymers and a lot of related articles were published. There are several reviews which emphasize on the different aspects of gas sensors (Dubbe, 2003; Zakrzewska, 2001; Timmer, 2005), and some others discussed in the sensing performance of certain conducting polymers (Nicolas-Debarnot, 2003; Maksymiuk, 2006; Ameer and Adeloju, 2005). However, only a few of the previous works gave special attention to summarizing the gas sensors based on different conducting polymers (Bai *et al.*, 2007).

### **1.3 Problem Statement**

Most of the work in semiconductor gas sensors focus on the optimum performance and good response between gas sensing elements with the selected sensing materials.

However, the main drawback of this type of gas sensor is the utilization of a higher operating temperature (greater than 200 °C) that will increase power

consumption and reduce sensor life. An interesting approach for lowering the operating temperature is by incorporating of organic materials as the sensing materials. It is known that the organic materials are fit to operate at low temperatures and have been applied in commercial devices but they are not stable enough in monitoring various types of gases such as reducing gases (Geng, 2009).

In the present study, the hybridization of the TiO<sub>2</sub> with the organic semiconductor materials as a gas sensor has been proposed. Organic materials such as conducting polymer could be integrated with the existing metal oxides since it is easy to be synthesized. Polyaniline (PANI) is a preferable conducting polymer among others and chemically sensitive besides has low conductivity despite of the poor mechanical properties. Therefore, it is a good approach to complement the characteristic of organic-inorganic sensing materials for the detection of acetone vapors along with the detection limit.

#### **1.4 Objectives**

The primary objectives of this research are:

- 1) To develop PANI-TiO<sub>2</sub> composite pellet using the in-situ chemical polymerization method.
- 2) To characterize the developed PANI-TiO<sub>2</sub> composite pellets using both chemical and physical analyses.
- 3) To study the effect of PANI loadings toward detecting of acetone vapor at various conditions.

- 4) To determine the optimum conditions (operating temperature and concentration of acetone vapor) of PANI-TiO<sub>2</sub> composite pellet toward detecting of acetone vapor.

## 1.5 Scope of Study

The preliminary study discusses the available metal oxide gas sensor (MOS), TiO<sub>2</sub> gas sensor in detecting reducing gas and acetone vapor. The performance of gas sensor was improved by identifying the selected conducting polymer which was used to attach with the preferable metal oxide, TiO<sub>2</sub>. The hybridization of these two components is based on the excellent behavior of conducting polymer at low operating temperatures with the well established TiO<sub>2</sub> gas sensor. They have good sensitivity, environmental friendly, easy to synthesis, cheap production cost and most commercialized in production (Tai *et al.*, 2010).

The aniline (ANI) was used as a monomer to form the polyaniline in addition of oxidizing agent, ammonium persulfate (APS) and hydrochloric acid (HCl) using in-situ chemical polymerization method. The synthesis of PANI-TiO<sub>2</sub> composite pellet was conducted at room temperature gaining emeraldine phase of polyaniline which is the most stable phase within the 2 hours of polymerization. The effect of the addition of PANI towards TiO<sub>2</sub> particles was studied and analyzed. The composite which was in powder form was further pelletized before preceding to characterization analyses and detection stage.

The PANI-TiO<sub>2</sub> composite pellet was characterized using X-ray Diffraction (XRD), Fourier Transformation Infrared Spectroscopy (FTIR), Transmission

Electron Microscopy (TEM) and Nitrogen adsorption-desorption surface analysis. Meanwhile for pellet form, the characterizations were carried out using Scanning Electron Microscopy (SEM) and Energy Dispersive X-ray (EDX) Spectroscopy.

The performance of PANI-TiO<sub>2</sub> composite pellet was measured using sensing measurement unit where two effects were studied. They were the effect of operating temperatures and the effect of acetone vapor concentrations. The optimum performance condition of PANI-TiO<sub>2</sub> composite pellet was identified using Design of Experiment (DOE) software.

## **1.6 Organization of The Thesis**

The thesis consists of five chapters and the detailed of each chapter is referring to the research study.

**Chapter 1** (Introduction) describes briefly on the general information on air pollution relates to the acetone emission which defines the properties of acetone, source of emission and impact to the environment and human. The contribution of inorganic and organic compound in the gas sensor is barely discussed and proceeded with the definition of gas sensor technology and types of mostly related gas sensor. This chapter also includes the problem statements of the research study which contribute to the approach of the proposed objectives in the current studies. The objectives are described in details in the scope of study and ended up with the organization of the thesis.

**Chapter 2** (Literature Review) encloses the reviews from previous researchers on gas sensor technologies. The discussion continued regarding the chosen of TiO<sub>2</sub> and PANI as raw materials and explains the utilization followed by the sensing materials characterization, sensing mechanism of acetone vapor towards PANI-TiO<sub>2</sub> composite and overall execution of composite sensor.

**Chapter 3** (Materials and Experimental Methods) explains the role of chemical reagents, experimental equipment and preparation method. The characterization of sensing materials and experimental set up are also studied and analyzed analytically.

**Chapter 4** (Results and Discussion) describes and analyses the results obtained from experimental observations. The results from characterization analysis are discussed while the effects on parameters of sensing materials preparation and detection activity are studied. The data optimization is analyzed using Design of Experiment (DOE) software and discussed in details followed by the discussion on the optimum performance of the sensing materials.

**Chapter 5** (Conclusions and Recommendations) concludes the overall research of this study in terms of data obtained and analyzed during the present study. The recommendations of the research are suggested and considered for future undertakings.

## **CHAPTER 2**

### **LITERATURE REVIEW**

#### **2.1 Introduction**

The gas sensor technology is mostly used in the application of gas detection as a safety precaution practically in environmental monitoring, automotive applications, industrial production control, sensor network and many other applications. For the last two decades, extensive efforts have not been compiled only for advancing these sensors but also for developing various types of new gas sensors, which have been in great demand to ensure safety, health, amenity, environmental reservation, energy saving and others (Yamazoe, 2005). Continuous development of sensor technology has been carried out where the performances due to some problems are improved from time to time.

This chapter generally reviews on matters related to the gas sensor technology with the specific aims to semiconductor metal oxide gas sensor and conducting polymer gas sensors. It also focuses on the reviews of gas sensing mechanism, type of composite gas sensor, type of conducting polymer, properties of gas sensor and method of preparation of gas sensor.

#### **2.2 Semiconductor Metal Oxide Gas Sensor**

Since 1962, it has been known that the absorption or desorption of a gas on the surface of a metal oxide changes the conductivity of the material. This phenomenon was first demonstrated using zinc oxide thin film layers (Seiyama *et al.*, 1962).

The target gas interacts with the surface of the metal oxide film (generally through the surface that adsorbed oxygen ions), which results in a change in charge carrier concentration of the material. The changes in charge carrier concentration serve an alteration of the conductivity (or resistivity,) of the material. The n-type semiconductor is the one in which majority charge carriers are electrons, and upon interaction with a reducing gas cause an increase in conductivity. Conversely, an oxidizing gas serves to deplete the sensing layer of charge carrying electrons, resulting in a decrease in conductivity.

The p-type semiconductor is a material that conducts with positive holes as the majority charge carrier, hence the opposite effects are observed with the material and showed an increase in conductivity in the presence of an oxidizing gas (where the gas has increased the number of positive holes). An increase of resistance with a reducing gas is observed where the negative charge introduced into the material reduces the positive (hole) charge carrier concentration. Different semiconductor metal oxide gas sensors have a different reading of resistance due to the type of gases detected.

Table 2.1: Sign of resistance change (increase or decrease) to change in gas atmosphere (William, 1999).

Classification	Oxidizing gases	Reducing gases
n-type	Resistance increase	Resistance decrease
p-type	Resistance decrease	Resistance increase

Band theory stated that within a lattice there exists a valence band and a conduction band. The separation between these two bands is a function of energy, particularly the Fermi level, defined as the highest available electron energy levels at

a temperature. Band theory for gas sensor is described in Figure 2.1. Insulators have a large gap between the valence and conduction band (typically taken to be 10 eV or more). As such a lot of energy is required to promote the electron into the conduction band and therefore, the electronic conduction does not occur. The Fermi level is the highest occupied state at  $T=0^{\circ}\text{C}$  (Shriver, 2006). Semiconductors have a sufficiently large energy gap (in the region of 0.5–5.0 eV) so that at energies below the Fermi level, conduction is not observed. Above the Fermi level, the electrons begin to occupy the conduction band, cause an increase in conductivity.

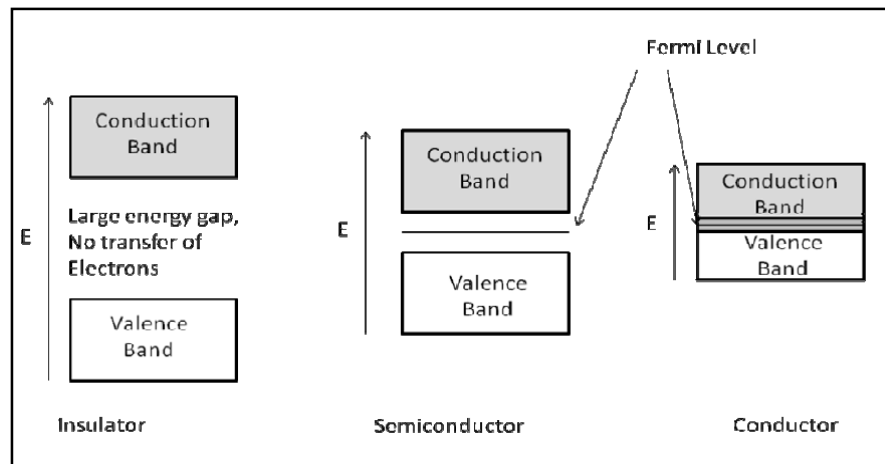


Figure 2.1: Schematic band diagrams of an insulator, semi-conductor and conductor. Note the small gap in the semiconductor, where electrons with sufficient energy can cross and the overlapping of the bands in the conductor (Shriver, 2006).

It is also highly desirable in the adsorption process for the metal oxide semiconductor sensors to have a large surface area to absorb as much as the target analyte on the surface, giving a stronger and more measurable response (especially at low gas concentrations). Production costs are kept low due to the simplicity of metal oxide semiconductor sensor devices. Their ability to be produced quickly and on a

large scale with easily controllable processes makes them a desirable technology to exploit. (Fine *et al.*, 2010).

### 2.3 Gas Sensing Mechanism

Gas sensing mechanism of semiconductor gas sensor is important to be understood in order to clarify the behavior of gas molecule during the interaction with oxygen ion. The detection activity varies at different temperature regions. Generally, there are two types of reaction occur on the pellet or thin film surface when flowing up the oxygen gas followed by the target gas.

#### i. Surface conductance effect.

Sensing phenomena mainly take place on the material surface sensor. Most of the reducing gases such as VOCs (ethanol, acetone and methanol), ammonia ( $\text{NH}_3$ ), carbon monoxide (CO), hydrogen ( $\text{H}_2$ ), nitrogen ( $\text{N}_2$ ) and others are used as target gases for gas sensor applications. In this case, the oxygen ( $\text{O}_2$ ) and carbon monoxide (CO) are chosen to explain the effect. The  $\text{O}_2$  molecules present in the atmosphere which are chemisorbed in the sensing material while the CO adsorbs oxygen (O) atoms from the surface of the material and becomes  $\text{CO}_2$ . This effect is much more preferable in the application of gas sensor according to the consideration on surface reaction rather than the bulk effect which is more complicated and limited (Spetz, 2006). Figure 2.2 illustrates the phenomena of surface conductance effects including oxygen, carbon and titanium atom by considering the reaction when flowing up the oxygen atom to the surface and forming oxygen species followed by the CO molecule which forms the  $\text{CO}_2$  molecule.

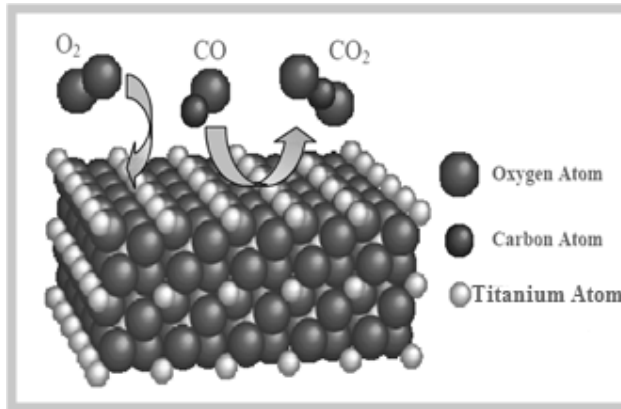


Figure 2.2: Surface conductance effect (Spetz, 2006).

ii. Bulk conductance effect.

Figure 2.3 shows the bulk conductance effect where the sensing phenomena take place inside the materials as the gas molecule penetrates the materials. It responds to the oxygen partial pressure changes in the upper temperature range (700°C and above) and reflects the equilibrium between the atmosphere and its bulk stoichiometry. This effect requires more time in order to produce the reaction and response (Spetz, 2006).

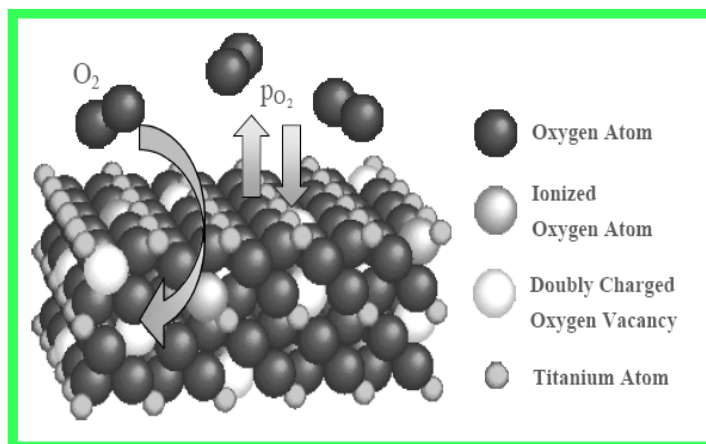


Figure 2.3: Bulk conductance effect (Spetz, 2006).

As mentioned earlier, the thick film is porous and non-stoichiometric in nature and has good interaction with the gas molecule due to the porosity and high surface area. Therefore, the oxygen chemisorptions centers, oxygen vacancies, localized donor and acceptor states and other defects have formed on the surface during synthesis. These centers are filled by adsorbing the oxygen from the air. The film interacts with the oxygen, by transferring the electrons from the conduction band to the adsorbed oxygen atoms, resulting in the formation of ionic species such as  $O^{2-}$  or  $O^-$  (Khayadate *et al.*, 2007).

The electrical conductivity occurs mainly through the grain boundaries and the oxygen molecule adsorbs on the surface of the metal oxide grain and picks up electrons which then forming oxygen ions. This gives the depleted region at the grain boundaries, which provides band bending in the materials, that is the resistivity of the material increases while for the conductivity, it will decrease at that condition (Spetz, 2006). The reaction mechanism is illustrated in the Figure 2.4.

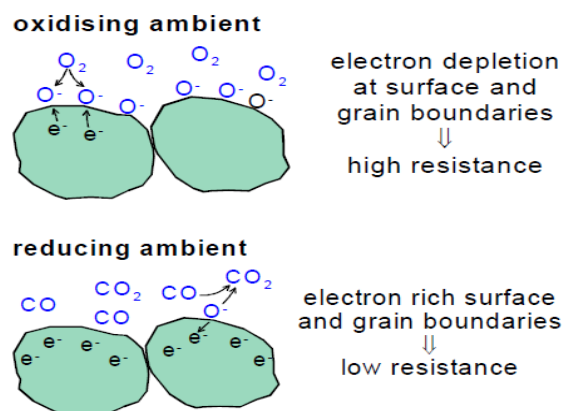


Figure 2.4: Schematic diagram of the sensing mechanism of the metal oxide semiconductor gas sensor (Spetz, 2006)

## **2.4 Composite Semiconductor Gas Sensor**

The composite semiconductor gas sensor is defined based on the combination or correlation between two types of materials forming gas sensor. From the previous discussion, the preferable metal oxide as semiconductor gas sensor is chosen according to the great performance in detecting gases especially for reducing gas. The correlation between metal oxide and other additional loadings will be discussed.

### **2.4.1 Metal-Metal Oxide Gas Sensor**

Nanocomposite films that consist of metal nanoparticles dispersed in a matrix of metal oxides have recently attracted much interest as the materials for gas sensors. Metal-metal oxide nanocomposites have physical properties that differ from those of the nanostructured single phase metal oxides. The metal nanoparticles play both passive and active roles in the sensing process. The presence of metal nanoparticles increases the active surface area and improves gas diffusion inside the film.

Metal nanoparticle also reduces the electrical resistance and increases the optical absorption of metal oxide. Metal nanoparticles such as platinum (Pt), palladium (Pd), gold (Au), and silver (Ag) also show catalytic properties that can modify the analyte–metal oxide chemical interactions and enhance the sensing process. The interfacial region between metal nanoparticle and metal oxide also has very different electron band structure than inside the bulk semiconducting metal oxide, which also contribute to the unique gas sensing properties of this type of nanocomposite (Yang, 2011).

## 2.4.2 Mixed Metal Oxides

Transition metal oxides can give good sensing performances due to their catalytic properties. Some transition metal oxides are stable and have low electrical resistance which enables them to operate at a low operating temperature, while others have high electrical resistivity and require high operating temperatures. Some of the oxides are more sensitive to the oxidizing gases while others are sensitive to the reducing gases. It is therefore a natural approach to combine metal oxides of different properties with an appropriate proportion so that the gas sensor performance can be modified as desired.

The gas response has been studied for SiO<sub>2</sub>- NiO and SiO<sub>2</sub>-SnO<sub>2</sub> nanocomposite films for H<sub>2</sub>, CO and humidity at different operating temperatures ranging from 25 to 350°C and gas concentrations between 10 and 1000 ppm. The SiO<sub>2</sub>-NiO and SiO<sub>2</sub>-SnO<sub>2</sub> nanocomposite films showed good responses with greater sensitivity to H<sub>2</sub> gas than CO in the whole range of operating temperatures (Martucci *et al.*, 2004; Martucci *et al.*, 2003a; Martucci *et al.*, 2003b).

The gas-sensing sensitivity, selectivity, and minimum detectable concentration toward different gases including acetone, CO, and NO<sub>2</sub> can be effectively controlled by different dopants and doping concentrations. The p-type NiO<sub>x</sub> doped TiO<sub>2</sub> shows high sensitivity towards ethanol and acetone with distinct behavior compared to other n-type TiO<sub>2</sub> thin films.

Siriwong (2009) reported that WO<sub>3</sub> doping significantly enhanced NO<sub>2</sub> gas sensing performance of ZnO nanoparticles. In addition, 0.5 mole% is found to be an

optimal  $\text{WO}_3$  concentration which gives the highest sensitivity towards  $\text{NO}_2$ . Other mixed oxides show the improved gas sensing properties include  $\text{Cr}_2\text{O}_3$ - $\text{WO}_3$  films for  $\text{NO}_2$  in  $\text{NO}_x$  mixtures (Cantalini *et al.*, 2004) and  $\text{Fe}_2\text{O}_3$ - $\text{ZnO}$  films for  $\text{NH}_3$  (Tang *et al.*, 2006).

### 2.4.3 Polymer-Metal or Metal Oxide

Metal oxide based gas sensors normally require high operating temperatures (300-500°C) (Toccoli *et al.*, 2003; Comini, 2006; Zhu *et al.*, 2004; Xiangfeng *et al.*, 2004; Khadayate *et al.*, 2007). High operating temperatures may lead to sensor instability and response variation. Sensors with low operating temperatures can inhibit structural change, reduce the power consumption and enables safer detection of combustible gases. Conducting polymers such as polypyrrole (PPy), polyaniline (PANI), polythiophene (PTh) and their derivatives typically can operate at low temperature in comparison to most of the metal oxide sensors. Conducting polymers can behave like semiconductors due to their heterocyclic compounds.

Mixing semiconductive metal oxide with PANI to form nanocomposites was found to be an effective way to improve the gas sensing properties of PANI (Tai *et al.*, 2007). It has been found that the nanocomposite exhibited higher sensitivity, faster response and recovery rates to  $\text{NH}_3$  than those of pure PANI thin film sensors fabricated under identical conditions. They found that the  $\text{TiO}_2$  components influenced the morphology of the nanocomposite film, which led to the variation of the sensor response-recovery behaviors.

Deshpande *et al.* (2009) discovered that good sensitivity, reproducibility and faster response to  $\text{NH}_3$  at room temperature can be achieved by using  $\text{SnO}_2$ -PANI nanocomposites films while under the same conditions pure  $\text{SnO}_2$  films remain inert. They found that the resistance of the nanocomposite ( $\text{SnO}_2$ -PANI) films decreased while pure PANI film resistance increased when exposed to  $\text{NH}_3$  which indicated that the  $\text{SnO}_2$  doping totally changed the electrical property of PANI.

## **2.5 Conducting Polymer Loadings on Metal Oxide**

Conducting polymers such as polyaniline, polypyrrole and polythiophene have been widely studied as the effective materials for chemical sensors. However, the drawbacks of these conducting polymers are low processing ability, poor mechanical strength and chemical stability (Matsuguchi *et al.*, 2003). There is a tremendous approach for the enhancement of the mechanical strength and characteristics of sensors by combining the organic materials with inorganic counterparts to form composites (Chuang and Yang, 2005; Sadek *et al.*, 2006).

### **2.5.1 Polyaniline**

Among the conducting polymers, polyaniline (PANI) is frequently used due to the ease of synthesis, environmental stability and intrinsic redox reaction (Chandrakanthi and Careem, 2002; Somani *et al.*, 1999; He, 2005). PANI can be found in three forms of oxidation states which are leucoemeraldine, emeraldine, and pernigraniline (refer Figure 2.5). Emeraldine is chosen to be the most useful form of PANI due to its stability at room temperature and it is electrically conducting upon doping with acids while leucoemeraldine and pernigraniline are poor conductors.

The efficient polymerization of aniline is achieved only in an acidic medium, where aniline exists as an anilinium cation. A variety of inorganic and organic acids of different concentration have been used in the syntheses of PANI which the resulting PANI, protonated with various acids, differs in solubility, conductivity, and stability (Levi, 2000). The handling of solid aniline salt is preferred for liquid aniline from the point of view of toxic hazards. Ammonium peroxydisulfate (APS) is the most commonly used oxidant, and its ammonium salt is preferred for the potassium counterpart due to its better solubility in water (Stejskal, 2002).

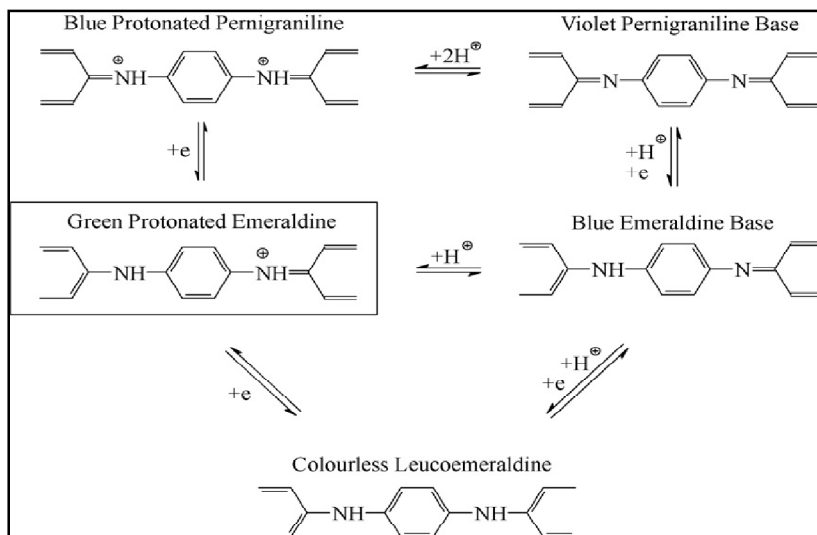


Figure 2.5: Protonated emeraldine obtained after the polymerization of aniline can be oxidized to pernigraniline or reduced to leucoemeraldine. Emeraldine and pernigraniline may be deprotonated to the corresponding bases (Stejskal *et al.*, 1996).

### 2.5.2 Polypyrrole

It is well known that PPy is a p-type conductive semiconductor. Upon exposure to the gas of an electron donor, a redox reaction occurs reversibly in PPy (Yang and Li, 2010). The PPy films thinner than 1 mm has different spectral properties depending on the conditions of synthesis and degree of PPy oxidation.

With the increasing degree, the color of the film changes from yellow to blue and, ultimately, black. The films have good adhesion to the substrate but at a thickness of over 10 nm they are easily peeled off from the electrode. The adhesion depends on a number of factors including the nature, coarseness, hydrophobicity of the electrode surface and the solvent used. The stability in the air of the doped PPy films is relatively high. Their degradation occurs only above  $150 \pm 300$  °C (depending on the dopant anion).

The surface of PPy films prepared in aqueous solutions looks like a cauliflower. The films synthesized in non-aqueous media and those with large organic anions have a smoother-looking surface. Polypyrrole is amorphous and usually gives only a diffuse halo in X-ray diffraction patterns. The electron diffraction shows that there are up to 15% (of total volume) of crystalline domains in the bulk of amorphous PPy.

## **2.6 Structure and Properties of PANI-TiO<sub>2</sub> Composite Gas Sensor**

### **2.6.1 Surface Morphology and Chemical Bonding**

The surface structure mostly relates to the sensing performance of gas sensor where the porous materials will be able to give high reaction rate during adsorption process. This is due to the fact that gas diffusion occurs more easily in porous structures, and the reaction between gas molecules and the thin film therefore occurs easily (Matsuguchi *et al.*, 2002).

Figure 2.6 shows the SEM analysis of the PANI/TiO<sub>2</sub> and PANI thin film surfaces synthesized using in-situ chemical polymerization and electrostatic self-assembly approach, prepared at 10°C (Tai *et al.*, 2008). The figure shows cylinder

like structure and there are many pores on the surface, which seem to contribute to the short response time and good reversibility of the sensors. The microstructure of the nanocomposite thin films is in good agreement with the sensor performance. Tai *et al.* (2010) reported that the sensor response is determined not only by the character of the polymer film, but also the morphology of the sensitive film. Meanwhile for the pellet structure, the TEM analysis is preferable instead of SEM analysis where it gives much clearer view on the structure of the materials as the pellet is considered bulk reaction on the adsorption.

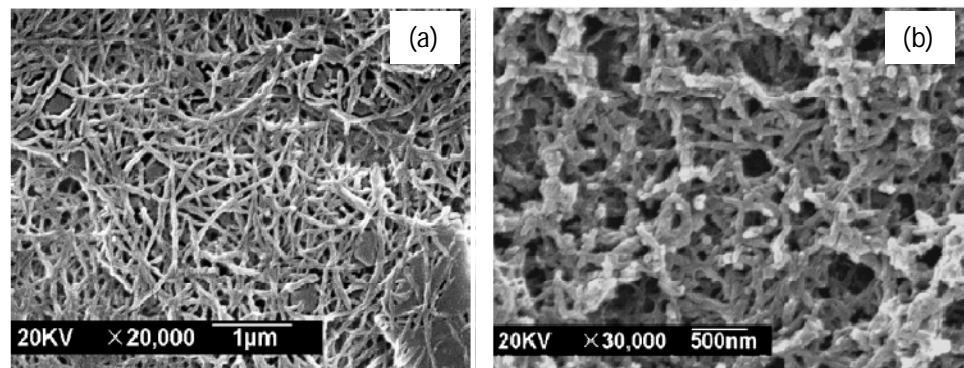


Figure 2.6: SEM image for (a) Pure PANI and (b) PANI:TiO<sub>2</sub> particles. (Tai *et al.*, 2008).

Figure 2.7 shows the TEM images where the structure of PANI within TiO<sub>2</sub> particles is clearer as the shape of PANI is amorphous and blurry boundaries. Electrical conductivity measurements indicate that the conductivity of composites at low loading of PANI is much higher than that of neat PANI, while with the increasing contents of PANI, the conductivity shows an orderly decrease (Xu *et al.*, 2005). Therefore, the composite sensor is predicted to give good performance at lower loading of PANI towards TiO<sub>2</sub> particles during sensing activity.

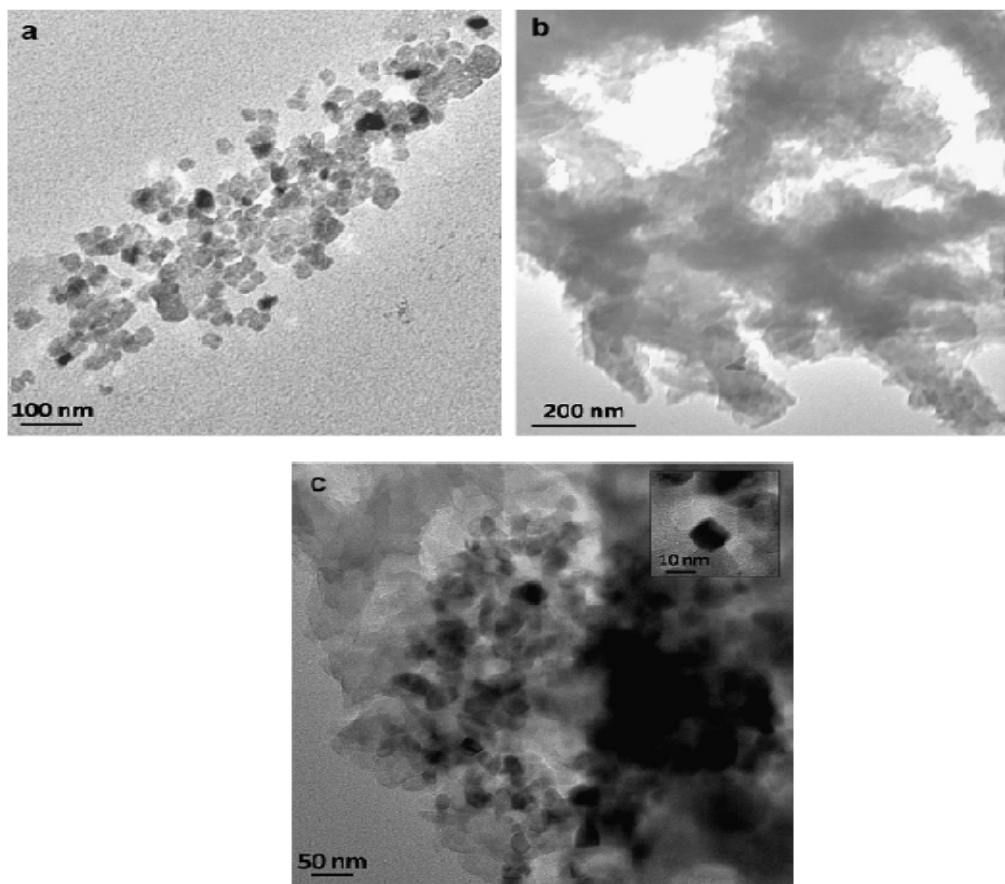


Figure 2.7: TEM images for (a) pure TiO<sub>2</sub>, (b) pure PANI, (c) PANI/TiO<sub>2</sub> composite (Srivastava *et al.*, 2011).

The chemical bonding exists within the composite has analyzed by using Fourier transformation infrared spectroscopy (FTIR). The chemical bond formed during the synthesis stage shows good interaction between those components and nicely joined each other as shown in Figure 2.8. The C=N and C=C bonds stretching modes for the quinonoid and benzenoid units of PANI peaks at 1400-1600 cm<sup>-1</sup>. The C-N bonds of the aromatic amines firm at band 1300 cm<sup>-1</sup>(Xu *et al.*, 2005) and the peak at 802 cm<sup>-1</sup> is assigned to the C-H bending vibration out of the plane of the para-disubstituted benzene rings (Geng *et al.*, 2007; Dutta and De, 2007; Li *et al.*, 2004). The O-H bonds formed at band near 1408 cm<sup>-1</sup> corresponds to the stretching